

# A stabilized Arlequin formulation for fluid-structure interaction analysis

Jeferson Wilian Dossa Fernandes<sup>1</sup>, Darcy Hannah Falcão Rangel Moreira<sup>1</sup>, Rodolfo André Kuche Sanches<sup>1</sup>

<sup>1</sup>*Dept. of Structural Engineering, School of Engineering of São Carlos, University of São Paulo  
Av. Trabalhador São-carlense, 400, São Carlos, São Paulo, Brazil  
jefersondossa@usp.br, darcyhannah@usp.br, rodolfo.sanches@usp.br*

**Abstract.** Fluid-structure interactions are multi-physical problems which may present complex coupled and localized phenomena. In the literature, most of the methods for these rely in two main approaches: interface tracking and interface capturing families of methods. In the interface tracking methods, fluid and solid discretizations are conform to the fluid-structure interface and its location is a part of the solution, requiring an additional step (mesh moving or re-mesh) when it changes. On the other hand, interface capturing methods employ immersed boundary techniques to describe the fluid-structure interface position in an Eulerian domain. In this work, an alternative approach is presented. Frame structures with Timoshenko-Reissner kinematics are modeled in the positional version of the finite element method, a simple alternative for the simulation of nonlinear dynamic problems. The fluid, described by the incompressible Navier-Stokes equations, is modeled in the Arlequin framework, a domain decomposition method based on the superposition of a local model (located in a particular region of interest) to a global one, unsuitable to capture the localized effects. The communication between models is provided by a Lagrange multiplier field, defined in a subset of the overlapping zone. This strategy has been applied successfully for the simulation of incompressible flow problems with fixed overlapped models, i.e., in an Eulerian description. In this work, the methodology is extended to an Eulerian-ALE version, covering the case of a moving local model, applicable to the simulation of fluid-structure interactions involving large structural displacements. The resulting model is coupled by a strong Dirichlet-Neumann partitioned scheme with Aitken's relaxation. Finally, flexibility and accuracy of our technique are evaluated by numerical tests. As main advantages, one can point the flexibility on the treatment of problems with large rigid body motion, such as turbines and rotors (a drawback of interface tracking methods, that sometimes requires re-meshing steps), while keeps a suitable discretization close to the fluid-structure interface throughout the analysis (not always possible when interface capturing methods are employed).

**Keywords:** Fluid-structure interaction, Domain decomposition method, Arlequin method, Stabilized finite elements.

## 1 Introduction

The main issue on solving fluid-structure interactions (FSI) concerns the couple of two physical problems usually described in different mathematical frameworks (Lagrangian for the structure and Eulerian for the fluid). From a geometric point of view, FSI problems can be classified regarding the treatment of the fluid-structure interface into two groups: interface capturing and interface tracking methods [1]. In the former, immersed boundary techniques are employed over Eulerian computational domains to track the interface position, which is usually performed by level-set functions and has proven to be more suitable for fluid-structure interactions with strong topological changes, such as large structural displacements. In interface tracking methods, the fluid-structure interface location is a part of the solution and the fluid discretization needs to be moved in order to represent the structural deformation. In this class of methods, the fluid governing equations are adapted to a consistent mathematical framework such as the Arbitrary Lagrangian-Eulerian (ALE) description [2] or Space-Time finite element approaches [3], which allows dealing with a moving computational domain. In both cases the fluid-structure coupling includes an additional step to the solution process: the fluid mesh update, which may be performed by several numerical approaches in order to keep a proper discretization avoiding excessive element distortion throughout the analysis, such as elasticity or spring analogy, Laplacian smoothing, among others.

However, both approaches present limitations. Interface tracking methods may need additional re-meshing

steps periodically, specially in cases when the excessive element distortion can no longer be avoided. On the other hand, in interface capturing methods it is not always possible to keep a suitable spatial discretization close to the fluid-structure interface. More recently, alternative techniques have been proposed to overcome such limitations based on the superposition of a localized fluid model close to the structure [4, 5]. Such approaches are developed in the sense of domain decomposition methods and have proven to be robust and precise on dealing with this class of problems, specially when the structure presents large displacements or rigid body motion.

In this work, we present a new methodology for the simulation of two-dimensional fluid-structure interactions involving large structural displacements in the context of domain decomposition methods. The FSI problem is solved in a strong Dirichlet-Neumann partitioned algorithm with Aitken's relaxation. The structure is modeled by frame elements with Timoshenko-Reissner kinematics in the positional version of the finite element method, a total Lagrangian framework developed by Coda and co-workers [6–8]. Finally, the fluid problem is solved by means of a stabilized version of the Arlequin method, presented in our previous work [9], and extended to the case of a moving overlapped model.

The paper is organized as follows: section 2 presents the fluid solver, based on a domain decomposition technique taking in account a moving overlapped model. Section 3 presents the structure solver and section 4 the fluid-structure coupling algorithm. A numerical example is presented in section 5 and concluding remarks are drawn in section 6.

## 2 Fluid solver

The Arlequin method is a domain decomposition technique based on the superposition of a local finite element model to a global one, so the localized effects can be properly approximated in a region of interest of the computational domain. In summary, the construction of an Arlequin-based formulation relies on three main principles: (i) the computational domain  $\Omega^f$  is built over the superposition of a local model  $\Omega_1^f$  to a global one  $\Omega_0^f$  and a sub-region of the overlapping zone ( $\Omega_{ov} = \Omega_0^f \cap \Omega_1^f$ ), named gluing zone ( $\Omega_c^f$ ), is defined; (ii) link the overlapped models by means of a coupling operator defined over  $\Omega_c^f$ , usually based on a Lagrange multiplier field; (iii) the energy distribution between models, in order to conserve the mechanical energy, guaranteed by a standard partition of unity basis function ( $\varrho_0, \varrho_1$ ) applied to the governing equations.

In our previous work [9], a methodology for the simulation of incompressible flows over a novel stabilized Arlequin formulation was introduced. In this work, we extend the stabilized Arlequin formulation to the case of a moving overlapped model in the context of fluid-structure interactions.

Consider the arbitrary computational domain  $\Omega_f$  at  $t = t_n$ , with global  $\Omega_0^f$  local  $\Omega_1^f$  models such that  $\Omega^f = \Omega_0^f \cup \Omega_1^f$  in a given position  $\mathbf{x}_{0(n)}$  and  $\mathbf{x}_{1(n)}$ , respectively. In the next time step  $t = t_{n+1}$ , the local model is moved to a new position  $\bar{\mathbf{x}}_{1(n+1)}$  in order to capture the structural displacement while the global model is kept unchanged. This kinematic is illustrated in Fig. 1.

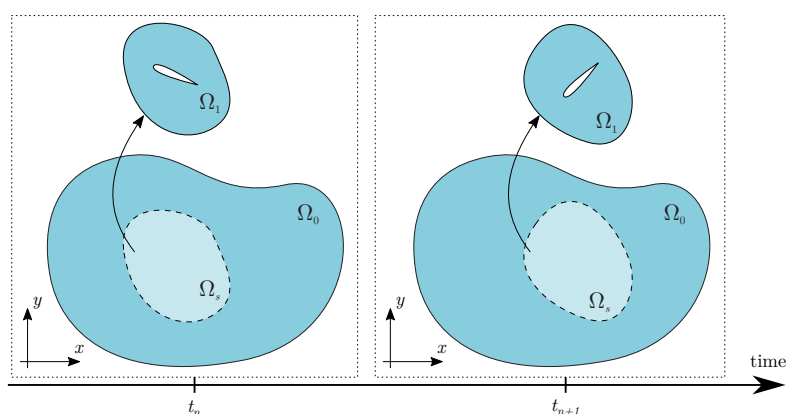


Figure 1. Arlequin Eulerian-ALE kinematics.

As pointed by [9], the Arlequin framework can be understood as the glue of two domains with different  $\varrho_i$  thicknesses, with velocity and pressure constants in the thickness direction. This assumption implies that there is no energy transport in the thickness direction.

Under such considerations, the two overlapped models can be analyzed separately in an Arlequin Eulerian-

ALE framework: the local model is modeled in the sense of ALE description and locally  $\varrho_1$  remains constant independently from the model motion; the Lagrange multiplier field, defined in a subspace of the local model, does not present energy transport when moved and no additional consideration needs to be provided; the global model geometry remains constant throughout the analysis and is modeled in an Eulerian framework, while the respective energy weight function  $\varrho_0$  needs to be updated and integrated over time, i.e.,  $\varrho_0 = \varrho_0(t)$ .

Thus, the problem of a flow modeled by the Navier-Stokes equations of incompressible flows in the Arlequin Eulerian-ALE framework may be written in within a stabilized finite element discretization as

$$\begin{aligned} & \int_{\Omega_0^f} \rho \varrho_0 \mathbf{w}_0^h \cdot \frac{\partial \mathbf{u}_0^h}{\partial t} d\Omega_0^f + \int_{\Omega_0^f} 2\mu \varrho_0 \boldsymbol{\varepsilon}(\mathbf{w}_0^h) : \boldsymbol{\varepsilon}(\mathbf{u}_0^h) d\Omega_0^f + \int_{\Omega_0^f} \rho \varrho_0 \mathbf{w}_0^h \cdot (\mathbf{u}_0^h \cdot \nabla) \mathbf{u}_0^h d\Omega_0^f \\ & - \int_{\Omega_0^f} \varrho_0 p_0^h \nabla \cdot \mathbf{w}_0^h d\Omega_0^f + \sum_{e=1}^{n_{el}} \int_{\Omega^e} \tau_{\text{SUPG}} ((\mathbf{u}_0^h \cdot \nabla) \mathbf{w}_0^h) \cdot \mathbf{r}_{M(0)} d\Omega_0^f \\ & + \sum_{e=1}^{n_{el}} \int_{\Omega^e} \nu_{\text{LSIC}} \nabla \cdot \mathbf{w}_0^h r_{C(0)} d\Omega_0^f + \int_{\Omega_c^f} \mathbf{w}_0^h \cdot \boldsymbol{\lambda}^h d\Omega_c^f = \int_{\Omega_0^f} \rho \varrho_0 \mathbf{w}_0^h \cdot \mathbf{f}_0^h d\Omega_0^f, \end{aligned} \quad (1)$$

$$\int_{\Omega_0^f} \varrho_0 q_0^h \nabla \cdot \mathbf{u}_0^h d\Omega_0^f + \sum_{e=1}^{n_{el}} \int_{\Omega^e} \tau_{\text{PSPG}} \left( \frac{\nabla q_0^h}{\rho} \right) \cdot \mathbf{r}_{M(0)} d\Omega_0^f = 0, \quad (2)$$

$$\begin{aligned} & \int_{\Omega_1^f} \rho \varrho_1 \mathbf{w}_1^h \cdot \frac{\partial \mathbf{u}_1^h}{\partial t} \Big|_{\bar{\mathbf{x}}_1} d\Omega_1^f + \int_{\Omega_1^f} 2\mu \varrho_1 \boldsymbol{\varepsilon}(\mathbf{w}_1^h) : \boldsymbol{\varepsilon}(\mathbf{u}_1^h) d\Omega_1^f + \int_{\Omega_1^f} \rho \varrho_1 \mathbf{w}_1^h \cdot ((\mathbf{u}_1^h - \bar{\mathbf{u}}_1^h) \cdot \nabla) \mathbf{u}_1^h d\Omega_1^f \\ & - \int_{\Omega_1^f} \varrho_1 p_1^h \nabla \cdot \mathbf{w}_1^h d\Omega_1^f + \sum_{e=1}^{n_{el}} \int_{\Omega^e} \tau_{\text{SUPG}} (((\mathbf{u}_1^h - \bar{\mathbf{u}}_1^h) \cdot \nabla) \mathbf{w}_1^h) \cdot \mathbf{r}_{M(1)} d\Omega_1^f \\ & + \sum_{e=1}^{n_{el}} \int_{\Omega^e} \nu_{\text{LSIC}} \nabla \cdot \mathbf{w}_1^h r_{C(1)} d\Omega_1^f - \int_{\Omega_c^f} \mathbf{w}_1^h \cdot \boldsymbol{\lambda}^h d\Omega_c^f = \int_{\Omega_1^f} \rho \varrho_1 \mathbf{w}_1^h \cdot \mathbf{f}_1^h d\Omega_1^f, \end{aligned} \quad (3)$$

$$\int_{\Omega_1^f} \varrho_1 q_1^h \nabla \cdot \mathbf{u}_1^h d\Omega_1^f + \sum_{e=1}^{n_{el}} \int_{\Omega^e} \tau_{\text{PSPG}} \left( \frac{\nabla q_1^h}{\rho} \right) \cdot \mathbf{r}_{M(1)} d\Omega_1^f = 0, \quad (4)$$

$$\begin{aligned} & \int_{\Omega_c^f} \boldsymbol{\zeta}^h \cdot (\mathbf{u}_0^h - \mathbf{u}_1^h) d\Omega_c^f + \sum_{e=1}^{n_{el}} \int_{\Omega_c^{f(e)}} \frac{\tau_{\text{ARLQ}}}{\rho} \nabla \boldsymbol{\zeta}^h : \nabla \mathbf{r}_{M(0)} d\Omega_c^f \\ & - \sum_{e=1}^{n_{el}} \int_{\Omega_c^{f(e)}} \frac{\tau_{\text{ARLQ}}}{\rho} \nabla \boldsymbol{\zeta}^h : \nabla \mathbf{r}_{M(1)} d\Omega_c^f = 0, \end{aligned} \quad (5)$$

where  $\rho$  is the fluid density and  $\mu$  the viscosity.  $\mathbf{f}_i^h$ ,  $\mathbf{u}_i^h$  and  $p_i^h$  with  $i = 0, 1$  are, respectively, the external force, velocity and pressure fields.  $\mathbf{w}_i^h$  and  $q_i^h$  with  $i = 0, 1$  refers to velocity and pressure test functions, respectively.  $\boldsymbol{\lambda}^h$  and  $\boldsymbol{\zeta}^h$  are the Lagrange multiplier field and its respective test function.  $\tau_{\text{SUPG}}$ ,  $\tau_{\text{PSPG}}$ ,  $\nu_{\text{LSIC}}$  and  $\tau_{\text{ARLQ}}$  are stabilization parameters (see [1, 9]) and  $\mathbf{r}_{M(i)}$ ,  $r_{C(i)}$  are the governing equations residuals.

Problem (1)-(5) is solved employing P2P2 finite elements to approximate all variables (velocity, pressure and Lagrange multipliers) for the spatial discretization and the generalized- $\alpha$  method [10] for the time marching.

### 3 Structure solver

Consider an arbitrary solid point, whose position are given by  $\mathbf{x} \in \Omega_x^s$  at the initial configuration ( $t=0$ ) and by  $\mathbf{y} \in \Omega_y^s$  at the deformed configuration ( $t = t_n$ ). From previous developments on the positional version of the finite element method (see e.g. [6, 7]) the dynamic equilibrium of a solid subjected to conservative loads can be written in a total Lagrangian framework as

$$\int_{\Omega_x^s} \rho_x \ddot{\mathbf{y}} \cdot \delta \mathbf{y} d\Omega_x^s - \mathbf{F} \cdot \delta \mathbf{y} - \int_{\Omega_x^s} \mathbf{b}_x \cdot \delta \mathbf{y} d\Omega_x^s - \int_{\Gamma_x^s} \mathbf{p} \cdot \delta \mathbf{y} d\Gamma_x^s + \int_{\Omega_x^s} \frac{\partial u_e}{\partial \mathbf{E}} : \frac{\partial \mathbf{E}}{\partial \mathbf{y}} \cdot \delta \mathbf{y} d\Omega_x^s = 0, \quad (6)$$

where  $\ddot{\mathbf{y}}$  refers to the solid acceleration,  $\rho_x$ ,  $\mathbf{F}$ ,  $\mathbf{b}_x$  and  $\mathbf{p}$  are the solid density and the vectors of concentrated, body and traction forces, respectively.  $u_e$  is the specific strain energy and  $\mathbf{E}$  the Green strain tensor, given by

$$\mathbf{E} = \frac{1}{2}(\mathbf{A}^T \mathbf{A} - \mathbf{I}) = \frac{1}{2}(\mathbf{C} - \mathbf{I}). \quad (7)$$

where  $\mathbf{A}$  is the deformation gradient, i.e.,  $\mathbf{A} = \nabla \mathcal{F}$  with  $\mathcal{F}$  being the mapping function and  $\mathbf{C}$  is the right Cauchy-Green deformation tensor. The last term in (6) refers to the strain energy and depends on the finite element kinematics, while the remaining terms are directly approximated by a standard finite element interpolation of positions.

In this work, frame structural elements are employed and, following the developments of [7, 8], its deformation can be mapped by means of a reference line and an auxiliary generalized vector on the nondimensional space  $\xi$ , as illustrated in Fig. 2.

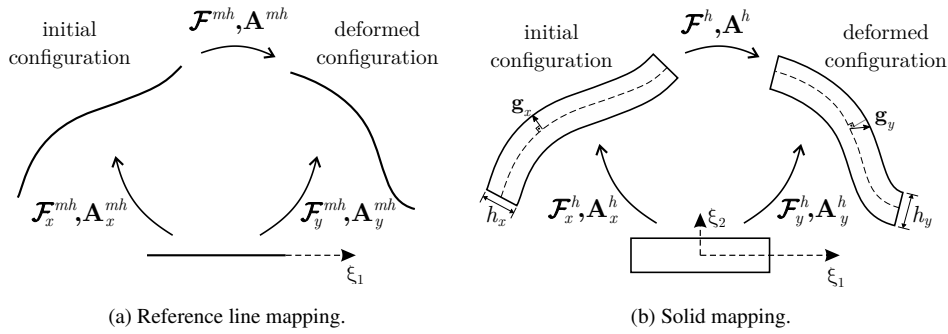


Figure 2. Frame finite element kinematics.

Thus, the complete solid mapping related to the nondimensional space for both initial and deformed configurations can be written, respectively, as

$$\mathcal{F}_x^h = \mathcal{F}_x^{mh} + \mathbf{g}_x = N_l(\xi_1)X_{li}^{mh} + \frac{h_x}{2}\xi_2 N_j(\xi_1)\mathbf{e}_{x(ij)}, \quad (8)$$

and

$$\mathcal{F}_y^h = \mathcal{F}_y^{mh} + \mathbf{g}_y = N_l(\xi_1)Y_{li}^{mh} + \frac{h_x}{2}[\xi_2 + a_j N_j(\xi_1)\xi_2^2]N_j(\xi_1)\mathbf{e}_{y(ij)}, \quad (9)$$

where  $N_l$  is the  $l$ -th shape function,  $X_{li}^{mh}$  and  $Y_{li}^{mh}$  are the  $l$ -th nodal coordinates in the  $i$ -th direction, respectively, in the initial and current configurations.  $\mathbf{e}_x$  is a unit vector in  $\mathbf{g}_x$  direction, orthogonal to the reference line in the initial configuration, and  $\mathbf{e}_y$  is a unit vector in  $\mathbf{g}_y$  direction, not necessarily normal to the reference line in the deformed configuration.  $h_x$  and  $h_y$  are the frame thicknesses in the initial and deformed configurations, respectively, and  $a_j$  is the  $j$ -th nodal value of strain rate along thickness.

Finally, the mapping from initial to the deformed configuration can be written as the composition of (8) onto (9), i.e.,  $\mathcal{F}^h = \mathcal{F}_y^h \circ (\mathcal{F}_x^h)^{-1}$ . Analogously, the deformation gradient is given by  $\mathbf{A}^h = \mathbf{A}_y^h (\mathbf{A}_x^h)^{-1}$ , where  $\mathbf{A}^h = \nabla \mathcal{F}^h$ ,  $\mathbf{A}_x^h = \nabla \mathcal{F}_x^h$  and  $\mathbf{A}_y^h = \nabla \mathcal{F}_y^h$ . These expressions allows to compute the Green strain tensor (7) and also the specific strain energy, adopted as a Saint-Venant-Kirchhoff material. Introducing these approximations onto the dynamic equilibrium expression (6) leads to a nonlinear problem of the type

$$\mathbf{M}\ddot{\mathbf{Y}} + \mathbf{F}^{int} = \mathbf{F}^{ext}, \quad (10)$$

where  $\mathbf{M}$  is the solid mass matrix,  $\ddot{\mathbf{Y}}$  is a vector of acceleration nodal values,  $\mathbf{F}^{int}$  and  $\mathbf{F}^{ext}$  are internal and external force vectors, respectively. Problem (10) is solved with cubic-approximation frame finite elements and the time marching is performed with the Newmark algorithm within a Newton-Raphson process.

## 4 Fluid-structure coupling

Fluid and structure solvers are coupled in an implicit partitioned scheme based on a fixed-point algorithm with Aitken relaxation [11]. At each time-step, the local model is moved to capture structural displacements. Following,

the fluid flow is updated and the flow dynamic loads are transferred to the solid. The structure solver is called and a new position of the fluid-structure interface is obtained and relaxed by the Aiten's relaxation parameter. This process is repeated until the interface position convergence, and the solution advances in time.

This procedure is summarized in Algorithm 1, where  $\mathcal{M}$ ,  $\mathcal{E}$  and  $\mathcal{F}$  refers to the fluid mesh, structure and fluid solvers, respectively.

---

**Algorithm 1** FSI time marching - fixed-point with Aiken relaxation

---

```

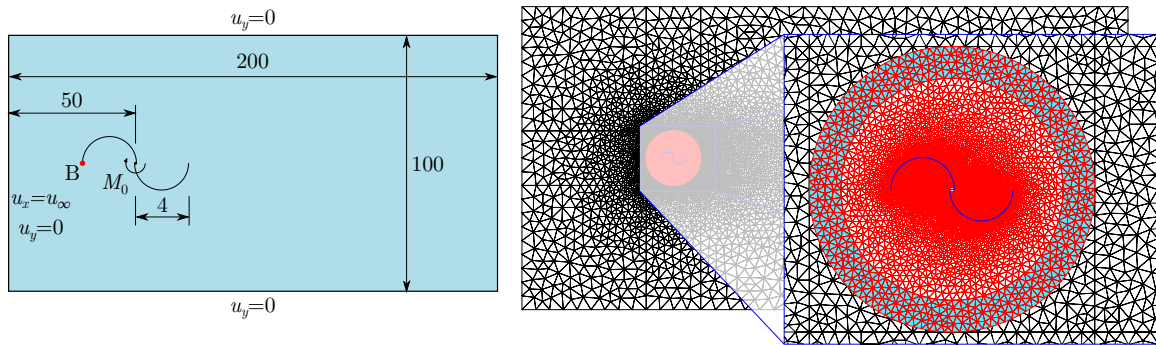
1: for every time step  $n$  do
2:    $k = 0$ ;
3:   - Predict the fluid-structure interface:  $\mathbf{x}_{n+1}^0 = \mathbf{x}_n + \Delta t \left( \frac{3}{2}\dot{\mathbf{x}}_n - \frac{1}{2}\dot{\mathbf{x}}_{n-1} \right)$  on  $\Gamma_{IFE}$ ;
4:   while ( $\epsilon >$  tolerance) do
5:     - Update the local model and compute the mesh velocity:  $\bar{\mathbf{u}}_1^k \leftarrow \mathcal{M}(\mathbf{x}_{n+1}^k)$ ;
6:     - Compute the trial interface position:  $\tilde{\mathbf{x}}_{n+1}^k \leftarrow \mathcal{E} \circ \mathcal{F}(\dot{\mathbf{y}}_{n+1}^{k-1}, \bar{\mathbf{u}}_1^k)$ ;
7:     - Compute Aitken's relaxation factor ( $\varsigma_{n+1}^k$ ):
8:     if  $k = 0$  then
9:        $\varsigma_{n+1}^0 = \varsigma_n^{k_{max}}$ ;
10:    else
11:       $\varsigma_{n+1}^k = \varsigma_n^{k-1} + (\varsigma_n^{k-1} - 1) \frac{(\Delta \mathbf{x}_{n+1}^{k-1} - \Delta \mathbf{x}_{n+1}^k) \cdot \Delta \mathbf{x}_{n+1}^k}{\|\Delta \mathbf{x}_{n+1}^{k-1} - \Delta \mathbf{x}_{n+1}^k\|}$ , where  $\Delta \mathbf{x}_{n+1}^k = \mathbf{x}_{n+1}^k - \tilde{\mathbf{x}}_{n+1}^k$ ;
12:    end if
13:    - Compute optimal Aitken's relaxation parameter:  $\varpi^k = 1 - \varsigma_{n+1}^k$ ;
14:    - Relax the interface position:  $\mathbf{x}_{n+1}^{k+1} = (1 - \varpi^k) \mathbf{x}_{n+1}^k + \varpi^k \tilde{\mathbf{x}}_{n+1}^k$ ;
15:    - Compute the fixed-point algorithm error:  $\epsilon = \|\Delta \mathbf{x}_{n+1}^k\|_{L^2} = \sqrt{\Delta \mathbf{x}_{n+1}^k \cdot \Delta \mathbf{x}_{n+1}^k}$ ;
16:     $k + +$ ;
17:  end while
18: end for

```

---

## 5 Numerical test

This example illustrates the robustness on solving practical engineering problems with the proposed formulation. It consists in a vertical axis Savonius-type wind turbine with two semicircular blades of 4cm diameter overlapped by 0.15 cm, as illustrated by Fig. 3. The structure is discretized by six finite elements of cubic approximation for each blade, connected by two additional straight and rigid finite elements, and composed by a material with Young's modulus  $\mathbb{E}=7 \times 10^7$  g/cm $\cdot$ s $^2$ , Poisson ratio  $\nu=0.33$ , thickness  $h_x=0.05$ cm and density  $\rho^s=2.7$  g/cm $^3$ .



(a) Geometry and boundary conditions (values in cm). (b) Local model (red), global model (black) and gluing zone (blue).

Figure 3. Numerical test: geometry, boundary conditions and fluid discretization.

The fluid domain geometry and boundary conditions are also presented in Fig. 3. The problem is modeled with a fluid with density  $\rho^f=1.18 \times 10^{-3}$  gm/cm $^3$  and viscosity  $\mu=1.82 \times 10^{-4}$  g/(cm $\cdot$ s). The flow inlet velocity is taken as  $u_\infty=20$  cm/s, corresponding to a Reynolds number equal to 1000, taking the turbine diameter as characteristic length.

The fluid computational domain is discretized by a global model with 16657 nodes and 8264 elements and a circular local model with 16724 nodes and 8198 elements. The gluing zone is taken as a strip 2cm wide at the

local model, corresponding to a discretization with 2164 nodes and 980 elements. The resulting Arlequin problem has 104471 degrees of freedom.

The analysis is carried with a time step  $\Delta t=0.002s$  and a constant impulsive initial torque of magnitude  $M_0=200 \text{ g}\cdot\text{cm}^2/\text{s}^2$ , removed at  $t=0.5s$ . During the simulation, point B displacement was monitored and the results are presented in Fig. 4.

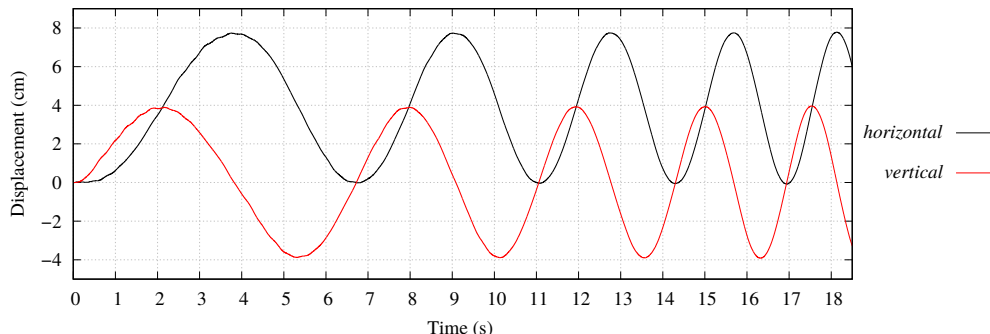


Figure 4. Numerical test: point B horizontal and vertical displacements history.

As can be noticed, after the initial impulse on the turbine, it presents an accelerated rotational motion due to the coupled phenomena developed by the structure rotation and the flow dynamic effects. The flow is characterized by a vortex shedding, which detach radially downstream from the turbine and may be observed in the snapshots of the velocity and pressure fields illustrated in Fig. 5 and 6.

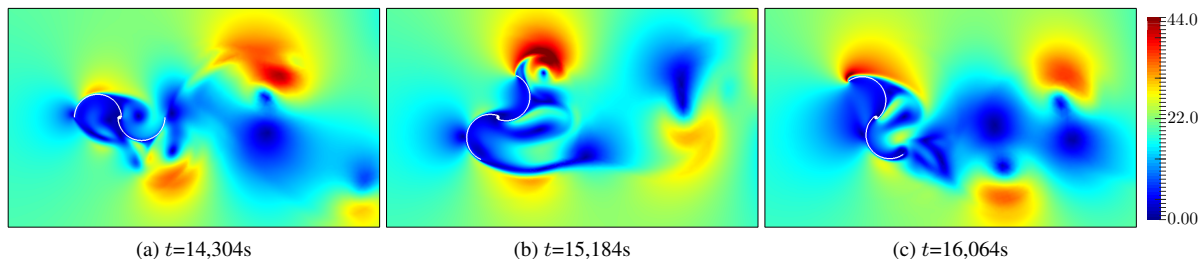


Figure 5. Numerical test: velocity field magnitude for a complete turbine rotation cycle. Values in cm/s.

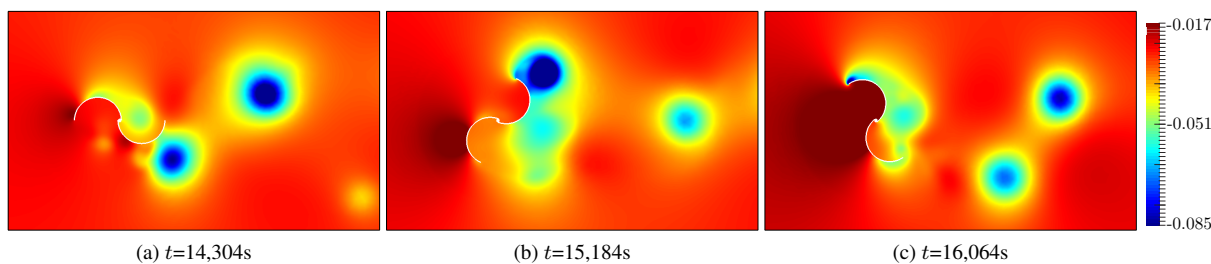


Figure 6. Numerical test: pressure field for a complete turbine rotation cycle. Values in  $\text{g}/\text{cm}\cdot\text{s}^2$ .

Although this example is not focused in a quantitative analysis, it illustrates the main advantages of our method. The magnitude of the rigid body displacement developed by the structure makes the analysis of this class of problems by means of conventional interface tracking techniques a challenging task, as it may require successive re-meshing steps. In addition, in the overlapping model methodology proposed in this work, the fluid local model discretization can be dynamically updated with minimal element distortion, as shown in Fig. 7.

## 6 Conclusions

In this work we presented a new methodology for FSI based on the superposition of a moving fluid model to a fixed one in order to represent the fluid-structure localized phenomena in two-dimensional problems. The

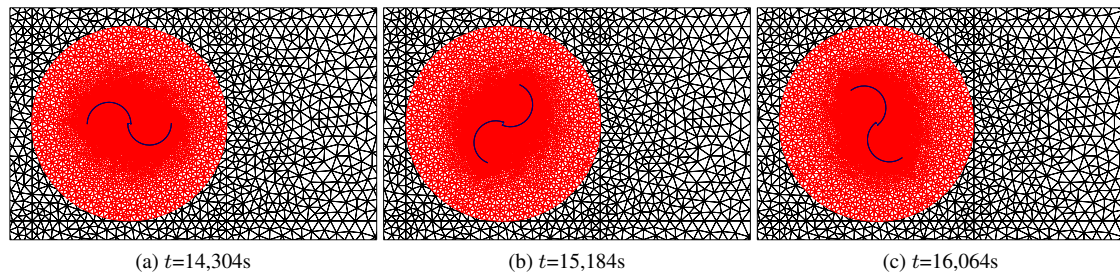


Figure 7. Numerical test: local and global models in a complete turbine rotation cycle.

communication between the overlapped models is performed in a stabilized Arlequin framework and this strategy have shown to be suitable for practical engineering computations, specially devices and mechanisms involving large displacements, as wind turbines, avoiding re-meshing and with a refined discretization always close to the fluid-structure interface. More realistic problems can be simulated with the extension of this formulation for three-dimensional problems, which we intend to explore in a future work.

**Acknowledgements.** This study was financed in part by the Coordenação de Aperfeiçoamento de Pessoal de Nível Superior – Brasil (CAPES) - Finance Code 001. The authors are also grateful to the Brazilian National Council for Research and Technological Development (CNPq).

**Authorship statement.** The authors hereby confirm that they are the sole liable persons responsible for the authorship of this work, and that all material that has been herein included as part of the present paper is either the property (and authorship) of the authors, or has the permission of the owners to be included here.

## References

- [1] Bazilevs, Y., Takizawa, K., & Tezduyar, T. E., 2013. *Computational Fluid-Structure Interaction: Methods and Applications*. John Wiley & Sons, Chichester, UK.
- [2] Donea, J., Giuliani, S., & Halleux, J. P., 1982. An arbitrary Lagrangian-Eulerian finite element method for transient dynamic fluid-structure interactions. *Computer Methods in Applied Mechanics and Engineering*, vol. 33, n. 1-3, pp. 689–723.
- [3] Tezduyar, T. E., Behr, M., & Liou, J., 1992. A new strategy for finite element computations involving moving boundaries and interfaces - the deforming-spatial-domain/space-time procedure: I. The concept and the preliminary numerical tests. *Comput. Methods Appl. Mech. Engrg.*, vol. 94, pp. 339–351.
- [4] Schott, B., Ager, C., & Wall, W., 2019. A monolithic approach to fluid-structure interaction based on a hybrid Eulerian-ALE fluid domain decomposition involving cut elements. *International Journal for Numerical Methods in Engineering*, vol. 119, n. 3, pp. 208–237.
- [5] Balmus, M., Massing, A., Hoffman, J., Razavi, R., & Nordsletten, D. A., 2020. A partition of unity approach to fluid mechanics and fluid–structure interaction. *Computer Methods in Applied Mechanics and Engineering*, vol. 362, pp. 112842.
- [6] Greco, M. & Coda, H. B., 2004. A simple and precise FEM formulation for large deflection 2D frame analysis based on position description. *Computer Methods in Applied Mechanics and Engineering*, vol. 193, pp. 3541–3557.
- [7] Coda, H. B., 2009. Two dimensional analysis of inflatable structures by the positional FEM. *Latin American Journal of Solids and Structures*, vol. 6, n. 3, pp. 187–212. ISSN 1679-7817.
- [8] Sanches, R. A. K. & Coda, H. B., 2016. Flexible multibody dynamics finite element formulation applied to structural progressive collapse analysis. *Latin American Journal of Solids and Structures*, vol. 13, n. 16, pp. 52–71.
- [9] Fernandes, J. W. D., Barbarulo, A., Ben Dhia, H., & Sanches, R. A. K., 2020. A residual-based stabilized finite element formulation for incompressible flow problems in the Arlequin framework. *Computer Methods in Applied Mechanics and Engineering*, vol. 370, pp. 113073.
- [10] Chung, J. & Hulbert, G. M., 1993. A Time Integration Algorithm for Structural Dynamics With Improved Numerical Dissipation: The Generalized- $\alpha$  Method. *Journal of Applied Mechanics*, vol. 60, n. 2, pp. 371–375.
- [11] Wall, W. A., Genkinger, S., & Ramm, E., 2007. A strong coupling partitioned approach for fluid–structure interaction with free surfaces. *Computers & Fluids*, vol. 36, n. 1, pp. 169 – 183.